

Improving Solar Cell System Performance using Fuzzy Logic MPPT Technique under Environmental Condition Variations

Mohamed El Amir Attalla

Electrical and Electronics Engineering,
Alexandria higher Institute of Engineering & Technology
(AIET)

Hassna M. El Arwash

Mechatronics Engineering ,
Alexandria higher Institute of Engineering & Technology
(AIET)

Abstract:- System life time, efficiency, cost and weight are among the most important goals for achieving sustainability for renewable energy systems. In order to reduce the cost and weight of the system, the Maximum Power Point Tracking (MPPT) technology is one method used to extract the maximum power up to 25% from the Solar Array (SA) used for small satellites as an example. The aim of this paper is to design a robust algorithm for MPPT controller taking into account trade-offs and rapidly changing environmental conditions such as Solar Irradiance (G), Temperature (T) and Air Mass Angle (Θ) as well as the splicing technology of cells in solar array system panels. The Fuzzy Logic Controller (FLC), as an intelligent control, is used in this approach for tuning the MPPT-fed duty cycle to control the boost DC-DC inverter. To achieve the applicability of the modelling results, MATLAB/Simulink is used for simulating external influences, describing system performance, in addition to programming Atmega16. The proposed system has been successfully implemented and tested on a PV assembly laboratory. The obtained experimental results clarified the functions and feasibility of the proposed control unit. Therefore, MPPT base on FLC is a practical controller to improve SA system efficiency under various environmental conditions.

1. INTRODUCTION

Solar energy is the most appealing system among renewable energy sources, and could be considered one of the worthiest sources as it has many pros including pollution-free as well as low operating and maintenance costs, which promise to grow its share in the near future. The world commission for environment and development described four key components of sustainability in relation to energy: capacity to scale. Energy supplies to meet growing human needs, energy efficiency and conservation, public health and safety, protect the biosphere and prevent further local pollution [1]. An international energy agency report that analyzed the world energy demand predicted that around 30 to 60 Terawatts of solar energy per annum will be expected by 2050 [2]. In solar energy systems, electrical energy is generated from the direct conversion of solar energy by solar photovoltaic (PV) modules. Solar cells, made of semiconducting materials, are the main component of solar PV systems (PVSs) [3, 4].

The performance of a PV framework is primarily influenced by three factors; the PV panel efficiency (between 8-23%), the efficiency of the inverter (approximately 95-98 %) and the maximum power point tracking (MPPT) technique efficiency (over 98%). Improving the performance of the PV panel and the inverter is not simple as it is constrained by the manufacturing technology and it might require better materials, which could dramatically increase the establishment cost. Instead, enhancing the tracking of the maximum power point (MPP) with new control techniques is simpler and not expensive, which lead immediately to rise the PV power generation and consequently to reduce its worth [5]. Due to the nonlinearly nature of the I-V characteristic curve of solar PV cells with the sun rays illumination and atmospheric temperature, it is necessary to have some methodologies to track peak current and voltage of the PV system to a specific operating point known as maximum power point (MPP) and, hence, peak efficiency at any climatic circumstances. So, it would be able to extract maximum solar energy which, in case of constant solar insolation and temperature, is traced by that characteristics curve. This strategy is recognized as maximum power point tracking (MPPT). That's why MPPT controller plays a vital role to boost up the output power obtained from the PV systems to its maximum value. However, various fast changing ecological conditions such as solar insolation, temperature, sunlight angle etc. affect the tracking efficiency of the MPPT controller [6].

Various MPPT technologies are available as suggested by many researchers who share their work in the academic literature [7-11]. Subudhi, et al. demonstrated a comparison between different MPPT techniques according to their classified types until January 2012. This study concluded a detailed description and classification of the MPPT techniques based on features, such as number of control variables involved, types of control strategies employed, types of circuitry used suitably for PV system and practical/commercial applications [7]. This survey could help future MPPT users in PV systems as a convenient reference. These researches did no one take into account different climate changes and their effect on the efficiency of solar cells.

In 2015, another survey was published by Bendib et al. in order to analyze, simulate, and evaluate a PV power supply system under varying meteorological conditions [8]. This paper provided a study on most MPPT techniques used in the PV systems, i.e., the perturbation and observation (P&O) method, the incremental conductance (Inc. Cond) method and the fuzzy logic (FL) based MPPT method. Within the context of this paper, numerical simulations (using Simulink/Mat lab) were carried out for PV systems containing conventional and intelligent fuzzy MPPT controllers, under varying climatic conditions. This survey considered only the temperature and irradiance changes not all the meteorological conditions. Moreover, it presented simulation study only to

ensure the effectiveness of fuzzy MPPT controller performances in terms of stability, precision and speed in the tracking of the MPP. The results showed much better performance than those of conventional MPPT methods (P&O and Inc. Cond).

In Ref. [9], the authors presented a comparative study among four popular techniques, which are the fixed duty cycle method, constant voltage (CV), perturb and observe (P&O), and incremental conductance (IC). Also, the paper considered some operational climatic conditions, i.e., irradiance and temperature only. This study concluded that the performance of the MPPT techniques has been analyzed by using a dc-dc buck converter supplying a resistive load. It can be seen that the obtained results do not imply significant error regarding the operation in MPP condition. In terms of efficiency, the analyzed methods presented good performance when compared with the fixed duty cycle method, which is not adequate for high power PV systems. IC algorithm has proven to be the best one, mainly because a significant increase in the extracted power is achieved.

Several MPPT methods have been studied and implemented in MATLAB/Simulink environment in Ref. [10]. Based on the generation of control signal, the MPPT methods have been proposed to be classified into three categories, i.e., conventional, Artificial Intelligence (AI)-based and hybrid methods. To study the considered MPPT methods with dynamic response for tracking the maximum power point, they are implemented in this PV system under varying solar irradiation conditions. Based on this study, a comparison of various classes of MPPT methods is carried out.

In Ref. 11, two MPPT techniques, i.e., Perturb and Observe algorithm (P&O) and Fuzzy Logic Controller (FLC), are used to control the photovoltaic systems to reach the maximum power point. Using the MATLAB program, a simulation of a 250 W photovoltaic module is realized to justify that the proposed FLC design accomplishes better performance than P&O technique under various radiances and temperatures. The results assured that FLC is faster than P&O-based MPPT system.

Adaptive Fuzzy Inference System (ANFIS) is a kind of Artificial Neural Network (ANN) that is based on the Takagi-Sugeno fuzzy inference system. Since it combines the concepts of ANN and FL, it has the potential to harness the benefits of both in one but with complex system [12].

The paper objective is to design a robust algorithm for MPPT controller considering trade-offs in the previous works and rapidly changing environmental conditions such as solar radiation (G), atmospheric temperature (T) and air mass angle (Θ). The effects of all environmental conditions are studied separately and together to reach the optimum performance for the MPPT controller. This is confirmed by a comparison with solar energy systems manufactured and operated in the field. The simulation was performed using MATLAB/Simulink and executing hardware prototype on Atmega16A with its designed software. The experimental results are confirmed and compared with manufactured devices and applied with cubic satellite. These results showed improved performance by reducing settling time and increasing accuracy.

2. MODELING AND SIMULATION OF PHOTOVOLTAIC ARRAY

2.1. Modeling of PV array

Firstly, an easy and accurate style of modeling PV arrays for various solar PV modules is adopted in this work. The basic Equation (1) depends on adding additional parameters to represent the practical PV device (array) mathematically, where the terminal current and voltage are related together as follows [13]:

$$I = I_{PV} - I_d = I_{PV} - I_0 [\exp (V+I R_s / a V_{th})-1] - (V+I R_s / R_p) \quad (1)$$

where I_{PV} and I_0 are the incident light-generated and p-n junction saturation currents of the PV array and $V_{th} = N_s k T / q$ is the array thermal voltage, where N_s is the number of series-connected cells per module.

The I_{PV} and I_0 currents depend on the effect of temperature and irradiance related to Equations (2) and (3) [13]:

$$I_{PV} = (I_{PV,n} + K_I \Delta T) G / G_n \quad (2)$$

$$I_0 = (I_{sc,n} + K_I \Delta T) / (\exp \{V_{oc,n} + K_V \Delta T / a V_{th}\} - 1) \quad (3)$$

where $I_{PV,n}$ is the I_{PV} at nominal/STC (usually 25 °C and 1 kW/m²), and as referred to [6] it is defined by:

$$I_{PV,n} = [(R_s + R_p) / R_p] * I_{sc,n} \quad (4)$$

$\Delta T = T - T_n$ is the change in the temperatures, where they are the actual (T) and nominal STC (T_n) ambient temperatures in °Kelvin).

G is the solar irradiation intensity on the PV array surface in Watt/m², G_n is the nominal STC solar irradiation intensity, K_V and K_I are the voltage and current temperature coefficients, respectively.

The value of the terminal current is obtained by iteratively numerically solving the I-V equation of (1), where for every V value, there is a corresponding I value that satisfies the I-V equation.

2.2. Maximum Power Point Tracking (MPPT) Algorithms

MPPT uses a specific tracking algorithm, whose basis is a control system and it is not considered as a mechanical tracking system. Although the two systems are totally different, the MPPT algorithm can be used in conjunction with a mechanical tracker system. Generally, MPPT controllers could be considered an essential and efficient part in photovoltaic systems. They possess the advantages listed below [14, 15]:

- They give more power (depending on weather conditions);
- They are more flexible, as they can have PV modules connected in series, in order to bring the voltage system up. This process reduces wiring gauge;
- They are cost effective, as they save transmission wiring required to install a PV system.

3. TEMPERATURE (T) AND IRRADIANCE (G) EFFECTS ON PV ARRAY

Equations from (1) to (4) and the input module parameters are combined together through MATLAB program to generate the electrical I-V/ P-V and R-V characteristics curves at different specified ambient temperature (T) in °kelvin and sun irradiation or insolation (G) in Watt/m² from the numerical solution of the current [16].

Basically, PV panel manufacturers' datasheets bring some of the parameters or specifications required for adjusting photovoltaic array models. The parameters available through datasheets are such as: $V_{OC,n}$ is the nominal open-circuit voltage, $I_{SC,n}$ is the nominal short-circuit current, V_{MP} is the voltage at MPP, I_{MP} is the current at MPP, K_V is the open-circuit voltage/temperature coefficient, K_I is the short-circuit current/temperature coefficient, and $P_{MAX,E}$ is the maximum experimental output power, as given in Table 1.

This information provided by datasheets is always extracted and commonly known as nominal conditions of ambient temperature and solar irradiation, however, some manufacturers' datasheets provide additional I-V characteristics curves for several irradiation and temperature conditions. The technique for evaluating the performance of a PV module is to compare the module performance against that provided by the manufacturer in the module's specifications under STCs.

Table 1: Specifications of the KC200GT PV Module at STC

I_{MP}	7.61 A
V_{MP}	26.3 V
$P_{MAX,E}$	200 W (+10%/-5%)
$I_{SC,n}$	8.21 A
$V_{OC,n}$	32.9 V
K_V	$-1.23 \times 10^{-1} \text{ V/}^\circ\text{C}$
K_I	$3.18 \times 10^{-3} \text{ A/}^\circ\text{C}$
N_s	54

3.1. Irradiance (G) Variations Effects on Electrical Characteristics Curves

For the selected PV module (KC200GT), the modeling algorithm expresses the resultant from MATLAB curves of the variations of irradiance level intensities that have great influence on the electrical characteristics' curves of the PV module. The irradiance levels taken into consideration are: 835W/m², 1000W/m² (that corresponds to the nominal isolation G_n) and 1350W/m².

3.2 Results for KC200GT PV Module at Temperature (T) of 25 °C

Figures (1) and (2) show how I-V and P-V curves change with irradiance level (G) when the ambient temperature remains constant for KC200GT PV module.

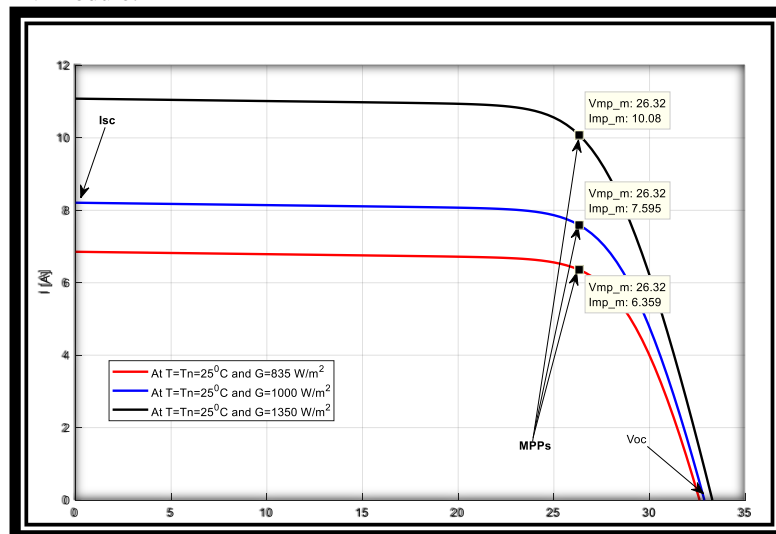


Figure 1: KC200GT I-V characteristics curve with different G at T of 25 °C

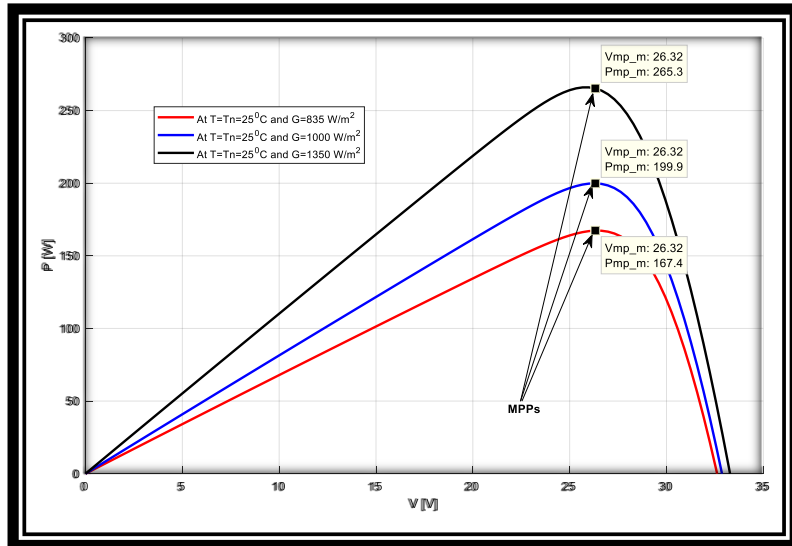


Figure 2: KC200GT P-V characteristics with different G at T of 25 °C

Upon Figure (1), the I-V curve show how the I_{SC} of PV arrays increases with solar irradiation level and it depends exclusively and linearly on the irradiance level. In addition, the V_{oc} increases slightly with the increase in irradiance level. It is of the order of **32.9 V** for 1 kW/m² of irradiance and 25 °C nominal temperature for multi-crystal KC200GT module. Furthermore, the current flowing through PV array increases with irradiance level. There is a direct proportional relationship between irradiance level and the output power of PV arrays as shown in Figure (2) of P-V curves for PV modules. In addition, the maximum output power increases with the irradiance level when the ambient temperature remains constant. The change in irradiance level leads to changes in voltage and current that specify the MPP.

3.3 Results for KC200GT PV Module with G of 1 kW/m² (AM1.5)

For PV module **KC200GT**, the simulation algorithm expresses the resultant from MATLAB curves of the variations of ambient temperature that have great influence on the electrical characteristics' curves of the PV module. The temperatures taken into consideration are: 25°C (that corresponds to the nominal temperature T_n), 50°C and up to 75°C. Figures (3) and (4) reveals how I-V and P-V curves change with ambient temperatures variations when the solar irradiance level remains constant for **KC200GT** PV module. The model important variables and points are highlighted in the figures.

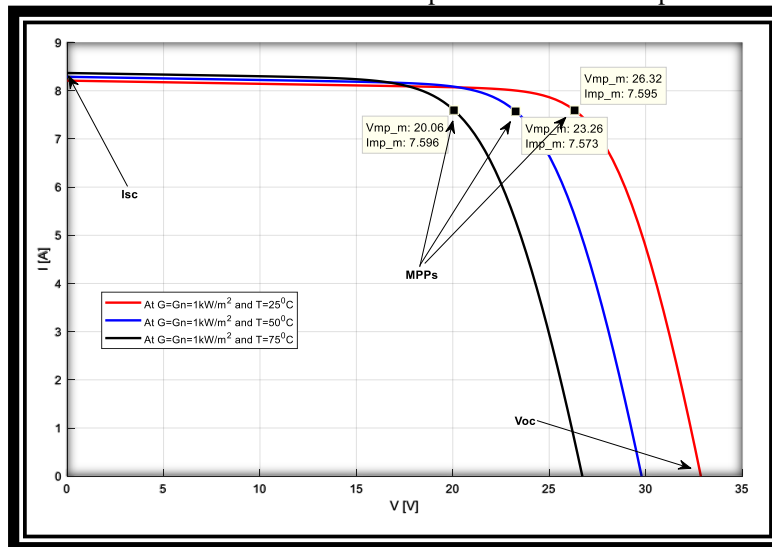


Figure 3: KC200GT I-V characteristics curve at T different with G of 1 kW/m²

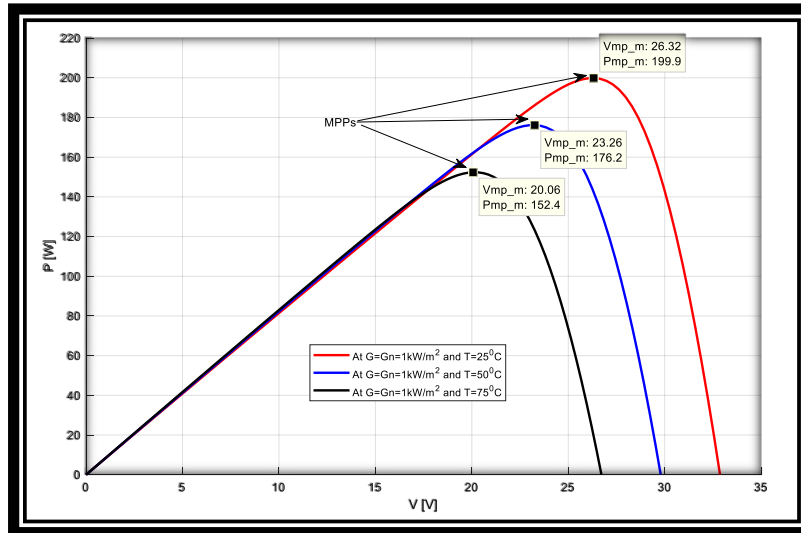


Figure 4: KC200GT P-V characteristics curve at different T with G of 1 kW/m²

The obtained results from the proposed model confirm the experimental and practical specifications of the selected PV module as recorded in the manufacturers' data sheets.

4. FLC-BASED MPPT AS CHARGE CONTROLLER

The MPPT controller method is used to operate PV panels at the point (MPP), due to its rapid response to the ecological conditions variability without being affected by PV array parameters changes. Also, FLC does not strictly require any knowledge of the exact mathematical model of the system. Additional benefits of fuzzy logic include its simplicity and its flexibility. It is very easy to be applied and implemented as it is based on system operation experience. Moreover, fuzzy logic simplifies dealing with nonlinearities of arbitrary complexity in systems and can handle problems with imprecise and incomplete data. The FLC examines the output PV power at each time sample (k), and determines the rate of change in the power relative to the voltage (dP/dV).

As it can be shown in Figure (5), it represents the idea of the rate of change variations over the P-V characteristics curve of the PV module. If this rate of change value is greater than zero, the FLC alters the D to rise the voltage until the power reaches its extreme or the dP/dV value equals zero. Otherwise, if this value is less than zero, the FLC alters the D to reduce the voltage until the power reaches its extreme or the dP/dV value equals zero.

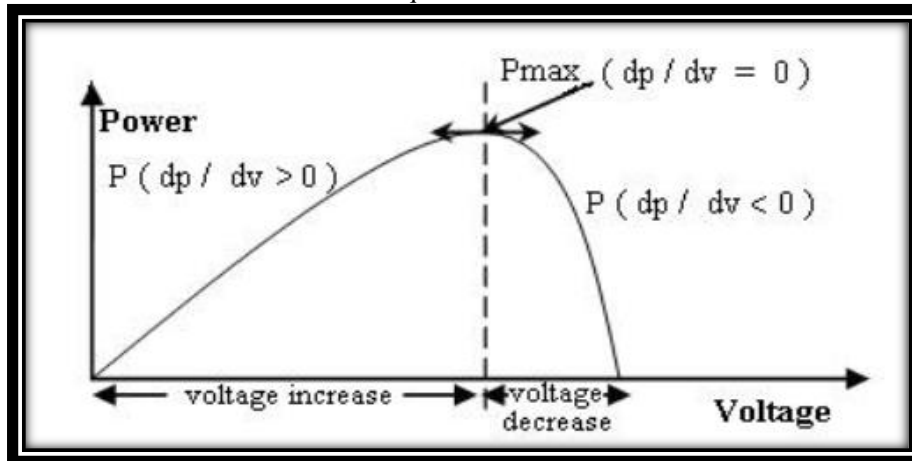


Figure 5: The dP/dV variability over P-V characteristics curve [17].

The two FLC input variables; Error, E(k), and Change in Error, CE(k) at sampled time k and they are modeled by Equations (5) and (6):

$$E(k) = [P(k)-P(k-1)] / [V(k) - V(k-1)] = \Delta P/\Delta V \tag{5}$$

$$CE(k) = E(k) - E(k-1) \tag{6}$$

where;

P(k): instantaneous power value of the PV array.

P(k-1): preceding power value of the PV array.

V(k): instantaneous voltage value of the PV array.

V(k-1): preceding voltage value of the PV array.

On one hand, the slope of the P-V characteristics curve is represented by the input $E(k)$, which defines the location of the load operation point at the instant k wherever it is situated on the left or on the right of MPP. On the other hand, the moving direction of this point to adjust the matching of the load operation point with the MPP is expressed by the input $CE(k)$.

The output variable of FLC is the change in duty cycle ratio ($CD(k)$), which can take positive or negative values relying on the location of the operating point on the P-V characteristics curve. The defuzzification method used in this model approach is the common center of gravity (COG) method that is well known as the centroid method or the center of area method (COA). It converts the fuzzy output of the inference mechanism to a crisp using membership functions into an analog signal. This output signal is fed to a PWM generator that controls the power DC to DC converter to the MPP that drives the load. Using the value of $CD(k)$ delivered by FLC, an accumulator is used to obtain the value of the duty ratio $D(k)$ in order to continue its cycle as shown in Equation (7).

$$D(k) = D(k-1) + C D(k) \tag{7}$$

Now, the designed FLC-based MPPT controller, that is represented by a subsystem, could be connected between PV array and DC-to-DC converter module to track the MPP for a complete loaded PV system, as shown in Figure (6).

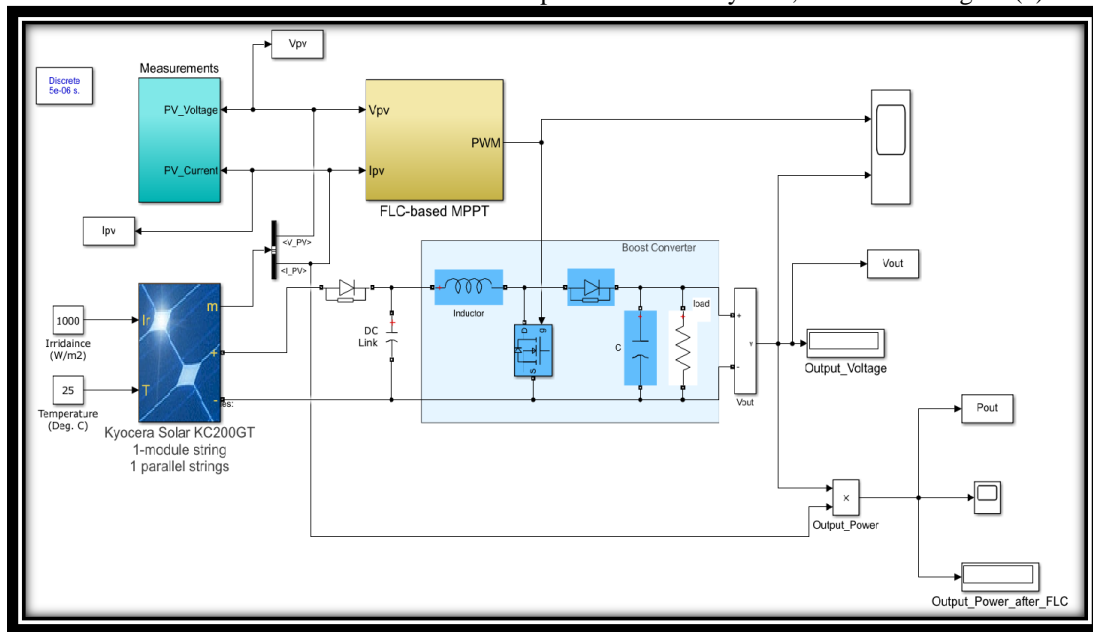


Figure 6: Simulink Model of PVS with FLC-MPPT and Boost DC-DC Converter

The PV array is represented by a Simulink function block that allows modeling of a variety of PV modules/arrays available from the national renewable energy laboratory (NREL) system advisor model [18].

5. SIMULATION RESULTS AND DISCUSSION

The complete PV matrix model is built into the Simulink model and the respective input parameters are prepared in the proposed approach. These parameters are the temperature of the atmosphere with different values in the range from 25 °C, the nominal temperature, - 75 °C and the solar radiation at different levels in the range from 835 W / m² to 1350 W / m² through the nominal isolation 1000 W / m². The average sampling time used in the simulation is 10⁻⁴ s. These settings are able to validate the PV matrix model by comparing both modeling and simulation results under the same conditions. The simulation is established on the KC200GT PV module for the modeling and their resultant curves. Figures (7) and (8) give the I-V/P-V characteristics curves, respectively, of the KC200GT PV module generated from the simulation in case of different G with nominal temperature T_n of 25 °C.

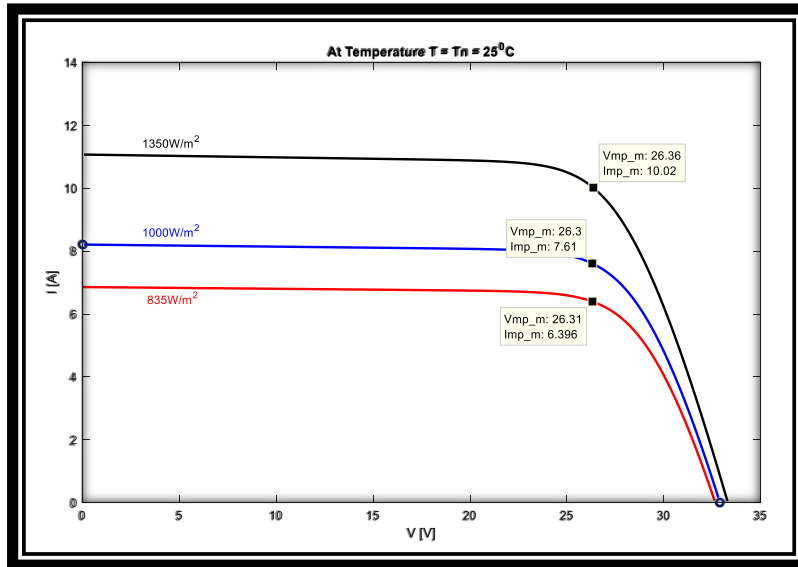


Figure 7: KC200GT Simulation's I-V characteristics curve with different G

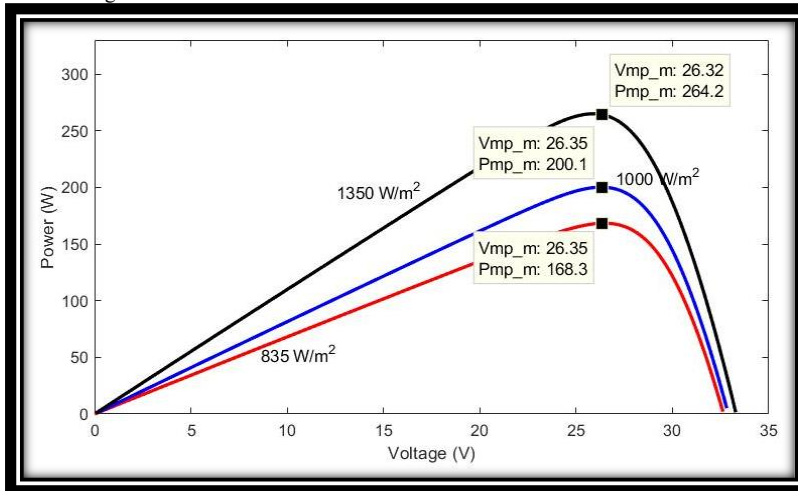


Figure 8: KC200GT Simulation's P-V characteristics curve with different G

Figures (9) and (10) give the I-V/P-V characteristics curves, respectively, of the KC200GT PV module generated from the simulation in case of different T with nominal irradiation (G_n) of 1 kW/m^2 .

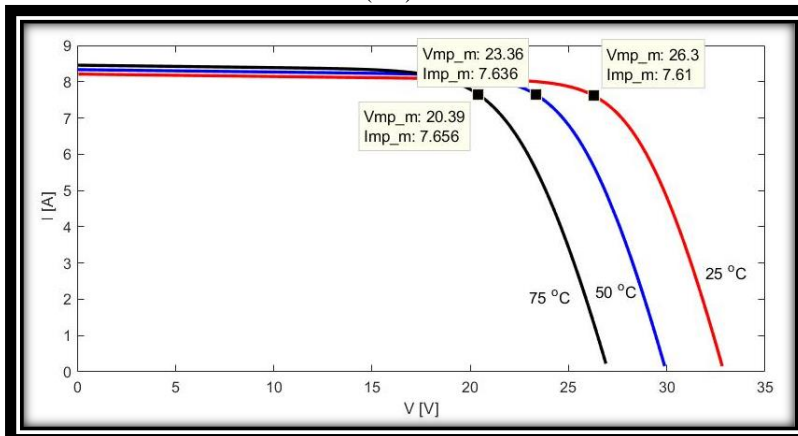


Figure 9: KC200GT Simulation's I-V characteristics curve with different T

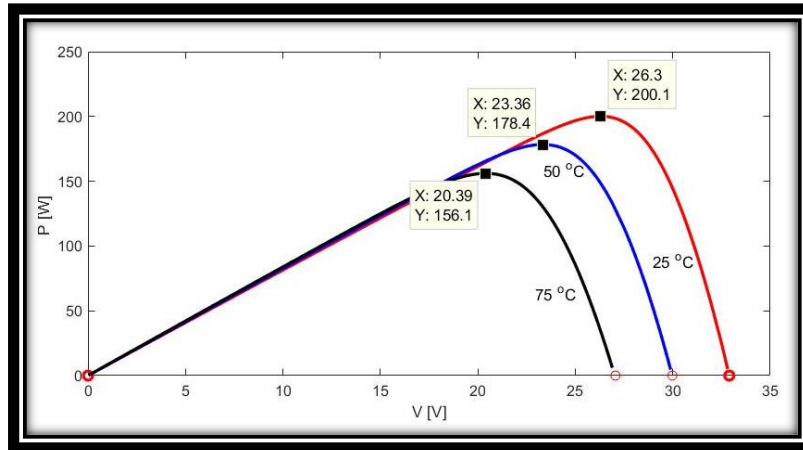


Figure 10: KC200GT Simulation's P-V characteristics curve with different T

6. SIMULINK MODEL OF THE FLC-BASED MPPT CONTROLLER

To test the performance of the PV system with the FLC-Based MPPT controller, different scenarios were simulated. Three scenarios that simulate changes in solar irradiance and sudden changes in operating ambient temperature of the PV array are presented.

6.1 Scenario 1: STC (Temperature of 25 °C & Solar Irradiance of 1 kW/m²)

In this case, the module is evaluated for nominal solar irradiance of 1000 W/m² and ambient temperature of 25 °C. V_{out} variations against time after applying the FLC-based MPPT algorithm are shown in Figure (11) for KC200GT PV module.

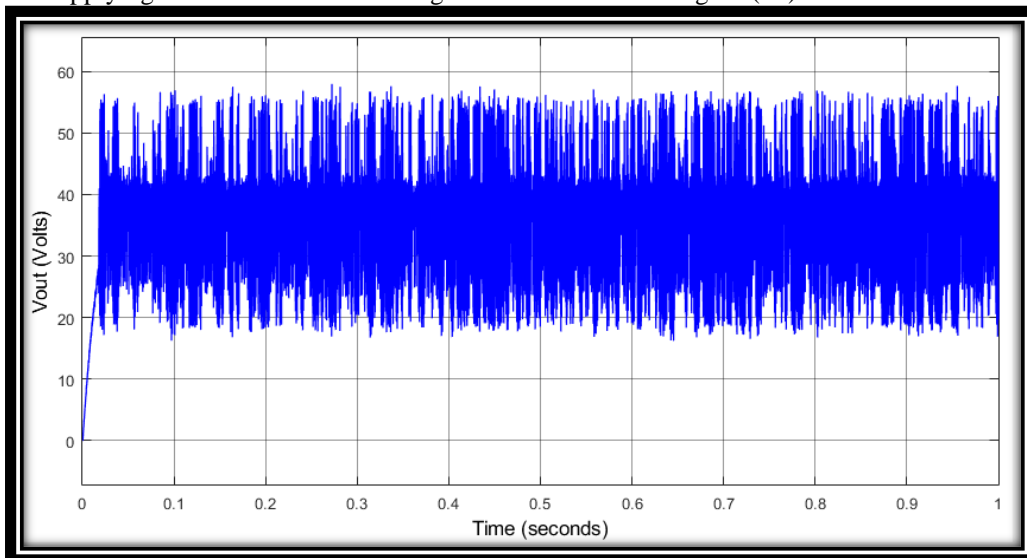


Figure 11 : V_{out} after FLC-Based MPPT for KC200GT PV System under STC

The above Figure (11) shows the change of output voltage with operating time in a fast response, and this is what distinguishes the proposed FLC-Based MPPT controller for the PV system as it is very sensitive to variations of the output voltage. It is capable of readjusting itself to maintain the stability of the PV system.

The output power (P_{out}) variations against time after applying the FLC-based MPPT algorithm are shown in Figure (12) for KC200GT PV module.

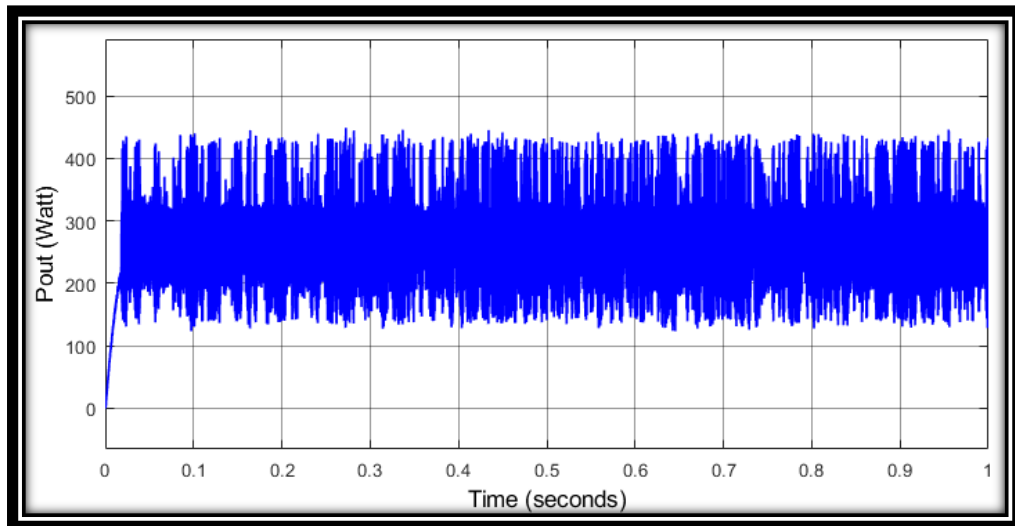


Figure 12: P_{out} after FLC-based MPPT for KC200GT PV System under STC

As a result of the change in the output voltage with time, rapid changes in the output power are consequently observed to achieve the stability of the PV system, which confirms the good performance as shown in Figure (12) for KC200GT PV module. This was clearly demonstrated through the use of the KC200GT PV module, which confirms the validity of the proposed model.

6.2. Scenario 2: Changes in Solar Irradiance at Temperature of 25 °C

In this case, the performance of the controller is evaluated with changes in solar irradiance on three states consecutively over the same time period, which are 835 W/m² then the nominal level 1000W/m² and finally 1350W/m² at fixed ambient operating temperature (T_n) of 25 °C as shown in Figure (13).

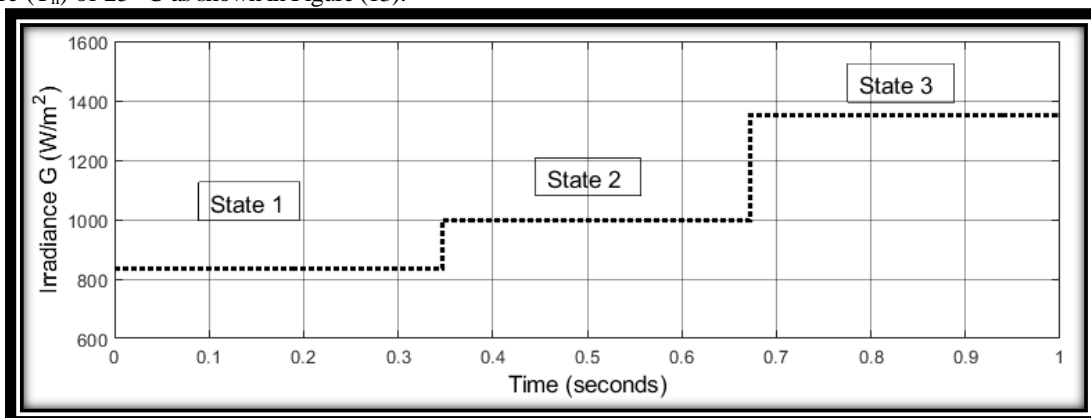


Figure 13: Irradiance Variation Levels with constant T_n

Figures (14) and (15) illustrate the irradiance variations effect on the V_{out} and P_{out} of the proposed FLC-based MPPT for the KC200GT PV system.

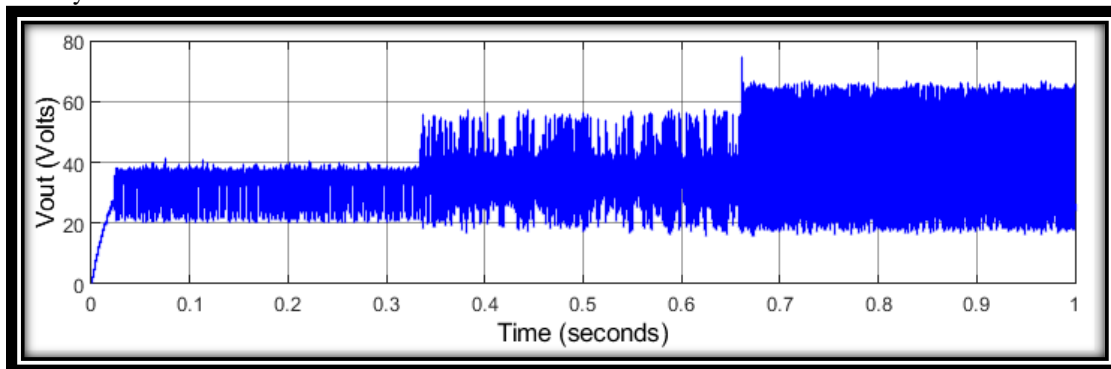


Figure 14: V_{out} after FLC-based MPPT for KC200GT PV System under various G and constant T_n

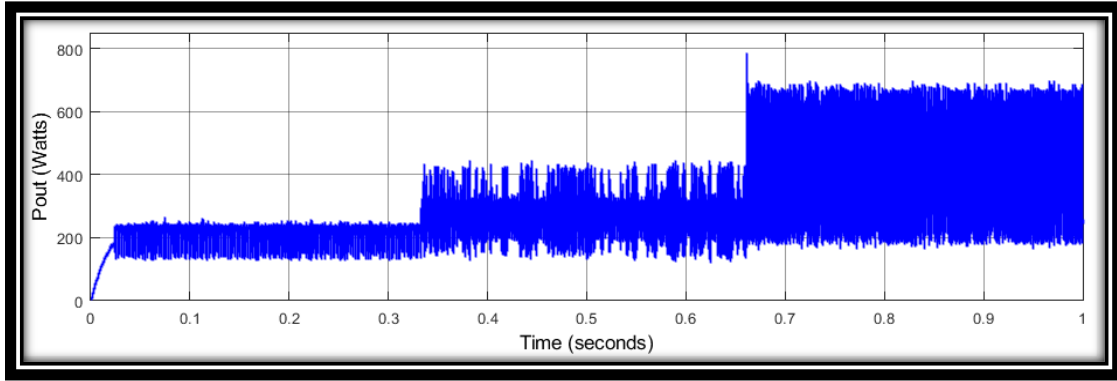


Figure 15: P_{out} after FLC-based MPPT for KC200GT PV System under various G and constant T_n

These figures show the variations of the output voltage and the output power with the operating time. At the low variation level of the irradiance (835 W/m^2), the output voltage variation response (ΔV_{out}) is relatively high. By increasing the irradiance levels from the range of 835 W/m^2 to 1350 W/m^2 , the speed response of the output voltage as well as the output power variations increase too. Hence, the speed response of the proposed PV system under varying solar insolation to reach its stability state is found to be fast enough. Consequently, the efficiency of the FLC-Based MPPT algorithm used to track the MPP rise from 94.8% to 99.4%.

6.3 Scenario 3: Changes in Temperature & Solar Irradiance of 1000 W/m^2

In this case, the performance of the system was evaluated for sudden changes in temperature such as the nominal 25°C , then 50°C and finally 75°C , all with a fixed ambient solar irradiance (G_n) of 1000 W/m^2 as in Figure (16).

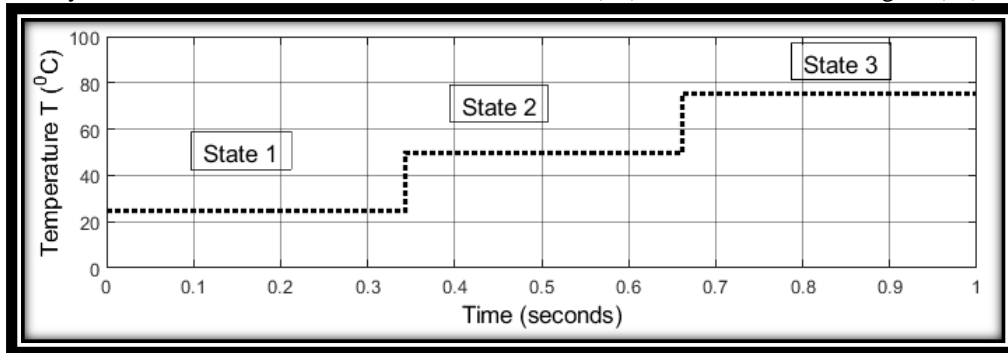


Figure 16: Temperature Variation Levels with constant G_n

Figures (17) and (18) illustrate the sudden temperature variations effect on the V_{out} and P_{out} of the proposed PV system for the KC200GT PV array under constant insolation.

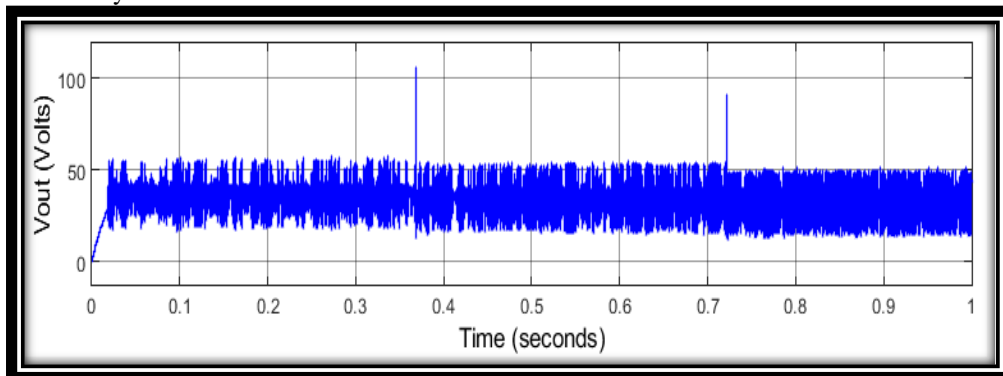


Figure 17: V_{out} after FLC-based MPPT for KC200GT PV System with different T and constant G_n

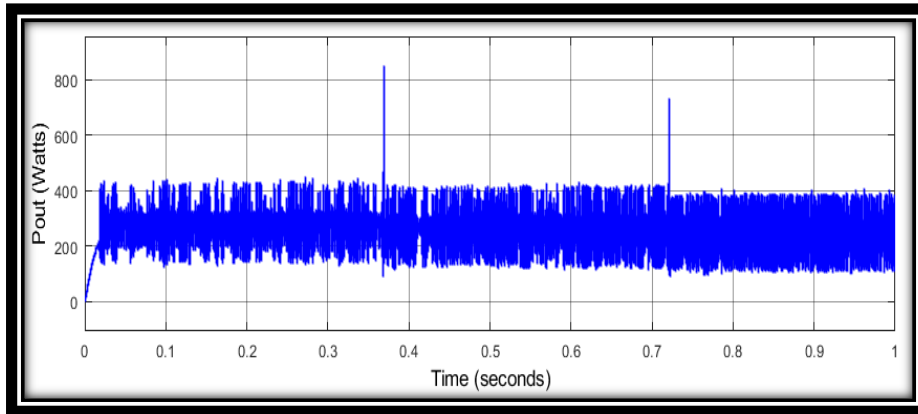


Figure 18: P_{out} after FLC-based MPPT for KC200GT PV System with different T and constant G_n

Figures (17) and (18) of the KC200GT array show the results of the three scenarios and the effect of changes in operating temperature on the V_{out} and P_{out} of the FLC based MPPT model. The effect of increasing the temperature on the V_{out} and P_{out} showed that the change is slightly slow and relatively small, as the proposed model performs suitable adjustments in order to achieve the optimum performance in real time for the PV system. Table 2 and Table 3 show comparisons between the mathematical model, simulation and the experimental datasheet for the two aforementioned used modules.

Table2: I-V/P-V Results & Specifications for MPPs at $T_n = 25^\circ\text{C}$ with different G for the KC200GT Module

	MATHEMATICAL MODELING	SIMULATION	EXPERIMENTAL DATASHEET
G=835 W/M2	$V_{MP} \approx 26.32 \text{ V}$	$V_{MP} \approx 26.32 \text{ V}$	$V_{MP} \approx 26.3 \text{ V}$
	$I_{MP} \approx 6.359 \text{ A}$	$I_{MP} \approx 6.396 \text{ A}$	$I_{MP} \approx 6.37 \text{ A}$
	$P_{MP} \approx 167.4 \text{ W}$	$P_{MP} \approx 168.3 \text{ W}$	$P_{MP} \approx 167.5 \text{ W}$
G = GN=1000 W/M2 (STC)	$V_{MP} \approx 26.32 \text{ V}$	$V_{MP} \approx 26.32 \text{ V}$	$V_{MP} \approx 26.3 \text{ V}$
	$I_{MP} \approx 7.595 \text{ A}$	$I_{MP} \approx 7.612 \text{ A}$	$I_{MP} \approx 7.61 \text{ A}$
	$P_{MP} \approx 199.9 \text{ W}$	$P_{MP} \approx 200.1 \text{ W}$	$P_{MP} \approx 200 \text{ W}$

Table 3: I-V/P-V Results & Specifications for MPPs at different T with $G= 1 \text{ Kw/m}^2$ for the KC200GT Module

	MATHEMATICAL MODELING	SIMULATION	EXPERIMENTAL DATASHEET
FOR T= 25 ° C	$V_{MP} \approx 26.32 \text{ V}$	$V_{MP} \approx 26.32 \text{ V}$	$V_{MP} \approx 26.3 \text{ V}$
	$I_{MP} \approx 7.595 \text{ A}$	$I_{MP} \approx 7.612 \text{ A}$	$I_{MP} \approx 7.61 \text{ A}$
	$P_{MP} \approx 199.9 \text{ W}$	$P_{MP} \approx 200.1 \text{ W}$	$P_{MP} \approx 200 \text{ W}$
FOR T= 50 ° C	$V_{MP} \approx 23.26 \text{ V}$	$V_{MP} \approx 23.36 \text{ V}$	$V_{MP} \approx 23.1 \text{ V}$
	$I_{MP} \approx 7.573 \text{ A}$	$I_{MP} \approx 7.636 \text{ A}$	$I_{MP} \approx 7.62 \text{ A}$
	$P_{MP} \approx 176.2 \text{ W}$	$P_{MP} \approx 178.4 \text{ W}$	$P_{MP} \approx 176 \text{ W}$
FOR T= 75 ° C	$V_{MP} \approx 20.06 \text{ V}$	$V_{MP} \approx 20.39 \text{ V}$	$V_{MP} \approx 20.3 \text{ V}$
	$I_{MP} \approx 7.596 \text{ A}$	$I_{MP} \approx 7.656 \text{ A}$	$I_{MP} \approx 7.63 \text{ A}$
	$P_{MP} \approx 152.4 \text{ W}$	$P_{MP} \approx 156.1 \text{ W}$	$P_{MP} \approx 154.3 \text{ W}$

7. EXPERIMENTAL SET UP

The hardware circuit prototype is shown in Figure (19). A prototype of the control system and the MPPT controller are implemented to validate the functionality of the proposed method by using Atmega16. They are used in serial or parallel connections to produce higher value of the power. Each type of configuration provides a special feature that might be useful depending on the application. In the current experiment, a PV module connected in series is used to achieve higher voltage.



Figure 19: Hardware circuit prototype

The experiments were conducted under radiation equal to approximately 1000 watts/m^2 and the temperature difference was from 25 up to $60 \text{ }^\circ\text{C}$, then the tests were repeated at a temperature of $25 \text{ }^\circ\text{C}$ and the radiation intensity varied from 835 watts / m^2 up to 1350 watts / m^2 , and the variation appeared in the form of the energy wave resulting. The variation in the output power waveform is shown in Figure (20). The proposed model performed suitable adjustments in order to achieve the optimum performance in real time for the PV system.

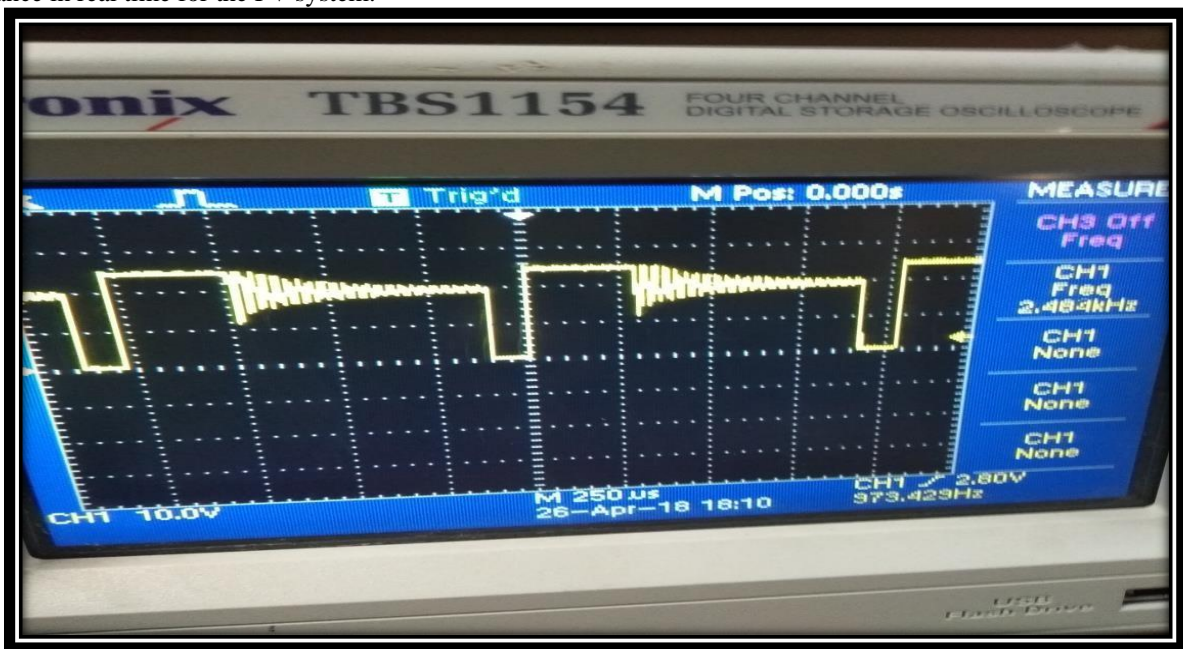


Figure 20: The output power wave generation for the hardware prototype experimental results

To verify the ability of the laboratory sample, a comparison is made with a MPPT controller operating in the field and through its datasheet, the accuracy of the results obtained from the prototype experimental result was confirmed with different environmental parameters. Table 4 shows a comparison of laboratory results and a real MPPT controller datasheet to demonstrate the quality of the experimental result.

Table 4. Performance indicators for the experimental results

Controller Parameters	Prototype experimental result	Datasheet value [19]
Rise time (t_r)	0.01 s	0.1 s
Settling time (t_s)	0.02 s	0.2 s
Over Shoot (OV)	5.1%	5 -7%
Ripple factor ($\Delta P/P$)	5.21 %	5.3 %

To study the applicability of the proposed technique, it is obligatory to test it with a real system. The experimental tests was carried out with the cubic satellite by installing the hardware prototype and a connection with solar cells installed on the satellite and testing it in different environmental conditions in terms of changing the temperature T, the irradiation G and changing the air mass angle Θ . The hardware prototype achieved excellent results in terms of settling time and high accuracy as shown in Table 4.

The results obtained demonstrate the ability of the designed MPPT system to track the appropriate voltage with the best response time of 0.02 s, along with the stability of the proposed and used algorithm.

7. CONCLUSIONS

As conformed in this paper, the PV module's output power and, consequently, the performance or the efficiency of the PV module are affected by the non-uniform solar irradiance and the variability of the atmospheric temperature. This is because any increases in solar irradiance will lead to increasing the short-circuit current, whereas any increases in temperature will lead to reducing the open-circuit voltage and, thus, the generated power varies too.

The simulation results prove that the fuzzy controller tracks the MPP and removes oscillations significantly and reduces power losses. The results comparisons show that the proposed design for the FLC-based MPPT provides better and fast dynamic response. It was demonstrated that the fuzzy controller has an excellent and robust performance when there are sudden changes in the operating temperature and solar irradiance levels for the PV system with the selected PV module.

The obtained results indicate that proposed and designed FL-MPPT controllers are capable of tracking the MPP while it is fast and accurate.

7. REFERENCES

- [1] P. Ashwini Kumari, P. Geethanjali "Parameter estimation for photovoltaic system under normal and partial shading conditions" *Renewable and Sustainable Energy Review*,(2018), 84, March: 1-11.
- [2] Zina, A. M.. "Study and Design of Stand-Alone Photovoltaic System to Maximizing Efficiency Solar Power Using Fuzzy Logic Algorithm", *International Journal of Computer Science Trends and Technology (IJCSST)*, (2018), 6(5): 92-94.
- [3] Samosir, A. S., Gusmedi, H., Purwiyanti, S., & Komalasari, E., "Modeling and Simulation of Fuzzy Logic based Maximum Power Point Tracking (MPPT) for PV Application", *International Journal of Electrical and Computer Engineering (IJECE)*, (2018), 8(3) : 1315-1323.
- [4] Hesan Ziar, Patrizio Manganiello, Olindo Isabella and Miro Zeman, "Photovoltaics: intelligent PV-based devices for energy and information applications" *Energy & Environmental Science journal*. (2020).
- [5] Rath, B. B., Kishore, T., Ramana, P. V., Prasad, P. R., & Saheb, S. P., "A Fuzzy Logic Control Based Maximum Power Point Tracker for a Stand Alone Solar Photovoltaic System under Uniform Radiation Condition". *International Journal of Multidisciplinary Research (IJMR)*, (2019), 5: 202-209.
- [6] Ulaganathan, M. S., & Devaraj, D., "A novel MPPT controller using Neural Network and Gain-Scheduled PI for Solar PV system under rapidly varying environmental condition", *Journal of Intelligent & Fuzzy Systems*, (2019), 37(1): 1085-1098.
- [7] Subudhi, B., & Pradhan, R. (2013). A Comparative Study on Maximum Power Point Tracking Techniques for Photovoltaic Power Systems. *IEEE TRANSACTIONS ON SUSTAINABLE ENERGY, VOL. 4, NO. 1*, 89 - 98.
- [8] Bendib, B., Belmili, H., & Krim, F. (2015). A survey of the most used MPPT methods: Conventional and advanced algorithms applied for photovoltaic systems. *Renewable and Sustainable Energy Reviews*, 637-648.
- [9] Tofoli, F. L., Pereira, D. d., & de Paula, W. J. (2015). Comparative Study of Maximum Power Point Tracking Techniques for Photovoltaic Systems. *International Journal of Photoenergy*.
- [10] Gupta, A., Chauhan, Y. K., & Pachaur, R. K. (2016). A comparative investigation of maximum power point tracking methods for solar PV system. *Solar Energy*, 236-253.
- [11] Mangeshkar, P. L., & Manohar, T. G. (2018). Design and Analysis of Optimal Maximum Power Point Tracking Algorithm using ANFIS Controller for PV Systems. *Asian Journal of Electrical Sciences*, pp. 100-106.
- [12] ARPACI, G. N., GÖZDE, H., & TAPLAMACIOĞLU, M. C. (2019). Design and Comparison of Perturb & Observe and Fuzzy Logic Controller in Maximum Power Point Tracking System for PV System by Using MATLAB/Simulink. *International Journal of Multidisciplinary Studies and Innovative Technologies*, pp 66 - 71.
- [13] Reisi, A. R., Moradi, M. H., & Jamasb, S., "Classification and comparison of maximum power point tracking techniques for photovoltaic system: A review", *Renewable and Sustainable Energy Reviews*, (2013), 19: 433-443.
- [14] Algarín, C. R., Giraldo, J. T., & Álvarez, O. R., "Fuzzy Logic Based MPPT Controller for a PV System", *Energies*, (2017), 10(12):2036.
- [15] Ibrahim, H., & Anani, N., "Variations of PV module parameters with irradiance and temperature", 9th International Conference on Sustainability in Energy and Buildings, energy procedia ,(July 2017), 134.
- [16] Villalva, M. G., Gazoli, J. R., & Filho, E. R., "Modeling and circuit-based simulation of photovoltaic arrays", *Brazilian Power Electronics Conference*, (2009), COBEP'09. Brazillian: 1244 - 1254, (2009).

- [17] Hamed, B. M., & El-Moghany, M. S., "Fuzzy Controller Design Using FPGA for Photovoltaic Maximum Power Point Tracking", (IJARAI) International Journal of Advanced Research in Artificial Intelligence, (2012), 1(3): 14-21.
- [18] Blair, N., Dobos, A. P., Freeman, J., Neises, T., Wagner, M., Ferguson, T, Janzou, S., "System Advisor Model, SAM 2014.1.14: General Description", National Renewable Energy Laboratory (NREL) at www.nrel.gov/publications, (2014).
- [19] https://www.google.com/search?sxsrf=ALeKk036DcgMm2CQ_vJgbVtDN-k4-0tpFw:1610044024125&q=data+sheet+for+manual+user+guide+of+mppt+solar+charge+controller